Influence of the direct exchange interaction on localization in a helical Kondo array

Einfluss der direkten Austauschwechselwirkung auf die Lokalisierung in einem helischen Kondo Array

Pol Alonso-Cuevillas Ferrer

Munich, 2017

Influence of the direct exchange interaction on localization in a helical Kondo array

Einfluss der direkten Austauschwechselwirkung auf die Lokalisierung in einem helischen Kondo Array

Pol Alonso-Cuevillas Ferrer

Bachelor Thesis
at the Faculty of Physics
of the Ludwig–Maximilians–Universität
Munich

submitted by
Pol Alonso-Cuevillas Ferrer

Munich, September 8, 2017

Supervisors:
Prof. Dr. Jan von Delft
Dr. Oleg Yevtushenko

Abstract

Edges of two-dimensional topological insulators are expected to have perfect ballistic conductance which is protected by physical symmetries. Experimentally, however, long samples show lower conductance and theoretical models explaining the experimental observations are highly needed. Altshuler, Aleiner and Yudson considered in Ref. [1] a chain of localized magnetic impurities at the edge of two-dimensional TIs with randomly anisotropic coupling of the electrons to the spins. This model was further expanded by Yevtushenko, Wugalter, Yudson and Altshuler in Ref. [2] where they considered effects of the electron-electron interaction. It was shown that such randomly anisotropic coupling could lead to spontaneous breaking of time reversal symmetry and to localization of edge modes. This model might explain suppression of the conductance discovered in the experiments. If the Kondo array is dense, the direct exchange interaction between the magnetic impurities may become important. In this work, we consider the effects of nearest neighbor $SU(2)$ symmetric Heisenberg interaction of the Kondo impurities on the edge transport and on the localization length. Our main result is that the localization length is not sensitive to the presence of this Heisenberg interaction.

Contents

1 Introduction

1.1 Topology in Condensed Matter Physics

When one speaks about topology, in a general sense, one refers to the field of mathematics describing the equivalence between spaces that can be smoothly deformed into one another. Two such spaces are considered to be topologically equivalent if such a smooth transformation is possible as is the case for the famous example of a doughnut and coffee mug. An important concept is that of topological invariants. These invariants are constructed in such a form that all topologically equivalent spaces have the same invariants. The most famous invariant is that of surfaces which is called the genus and corresponds to the number of holes, so a doughnut and a coffee mug are equivalent because they both have one hole, but they are different than a sphere which has none. The idea of topology is extended to condensed matter physics. Let us consider a zero-dimensional example [3], an N-state quantum dot weakly coupled to a metallic lead through a potential barrier, so that we are able to identify the states in the dot in respect to the chemical potential μ at $E = 0$: positive energy levels correspond to empty states and states below zero-energy are fully filled. Note that in this zero-dimensional example the energy levels correspond to single particles, but these concepts can easily be generalized to band theory, where we would be talking about the valence and conducting bands respectively. Restricting ourselves to non-interacting single-particle Hamiltonians, we now ask whether two such Hamiltonians can be deformed into one another. This question has a positive answer when one considers any two Hamiltonians of the same size, see Fig. 1, because it is always possible to connect the different energy states. It is only after we impose a further restriction to the transformation that we are able to define what it means for two Hamiltonians to be considered topologically equivalent.

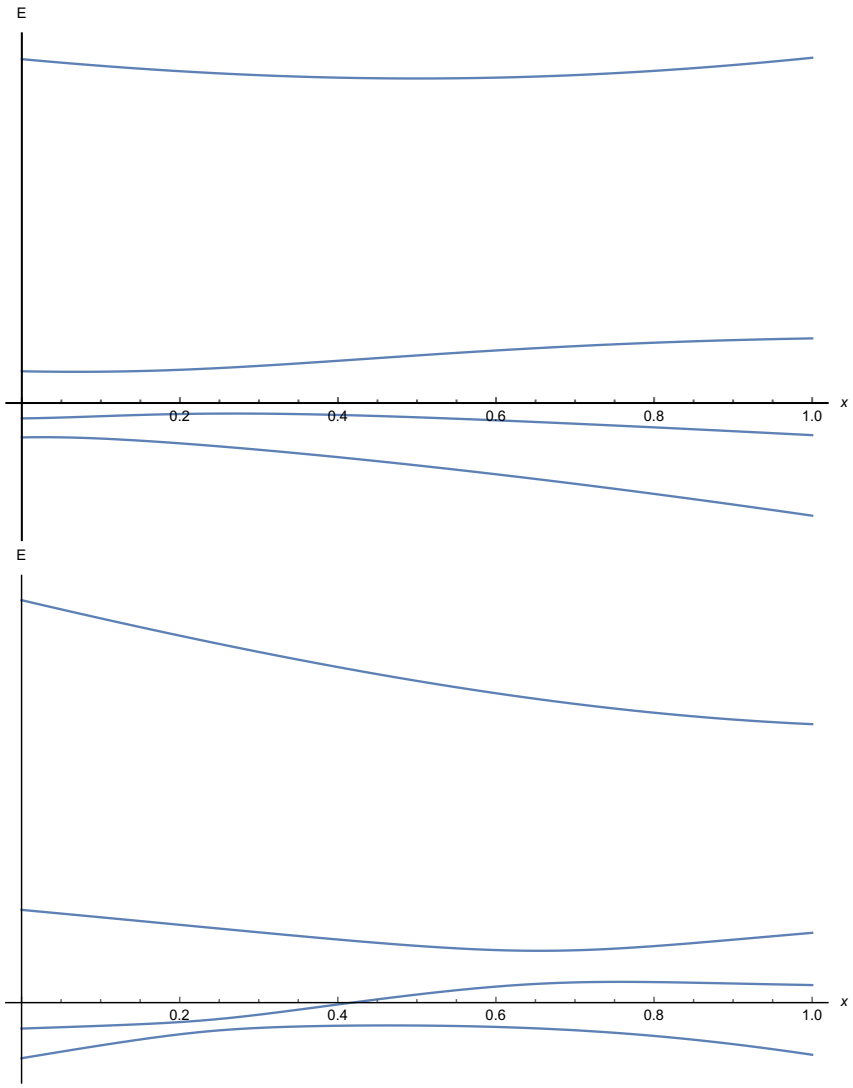

Figure 1: *These two graphics represent a possible transformation between the eigenvalues of two different pairs of randomly generated 4x4 Hamiltonian at x=0 and x=1. Two systems are topologically equivalent if they the can be adiabatically connected without closing the global gap. The upper panel shows two topologically equivalent systems. The lower panel shows two systems that are not topologically equivalent.*

For this matter, we restrict ourselves to gapped systems, i.e. systems that have a finite distance between the last filled energy level and the first empty one and we impose the rule that the transformation from one Hamiltonian to another may not close a finite global gap corresponding, for example, to the size of thermal excitations.

This rule states that the upper panel of Fig. 1 represents two topologically equivalent systems whereas the lower panel represents two systems that are not topologically equivalent. We now ask whether there is a topological invariant that tells us whether two Hamiltonians are topologically equivalent. Indeed in order for the global gap not to be closed, both Hamiltonians need to have the same number of negative energy states, which means that the transformation will necessarily have the same number of zero-energy crossings from below as from above. We thus find that zero-dimensional topologically equivalent states can be described with a $\mathbb{Z}$ invariant corresponding to the number of zero-energy crossings, for systems with general Hamiltonians with no further symmetries than hermicity. If one considers Hamiltonians with some symmetry the situation might change. An example is time-reversal symmetry (TRS). Kramers degeneracy [4, 5] tells us, that under TRS, for half-integer spin systems, there is an even number of degenerate states for every energy state. We can thus imagine every zero-energy crossing in Fig. 1 as changing the topological invariant by at least two. Such a system has, therefore, a $2\mathbb{Z}$ topological invariant, since the number of zero-energy crossings is always even. This consideration can be generalized to higher dimensions and by considering further symmetries [6–9]. Such a generalization has been done following Atland and Zirnbauer's (AZ) classification scheme for random matrices [10] and considering TRS, particle-hole symmetry (PHS) and chiral symmetry (CS). The possible topological invariants for d dimensions is represented in Tab. 1. Marked in yellow are the two zero-dimensional states considered above for no symmetries and for half-integer valued spin systems under TRS (i.e. $\Theta^2 = -1$, where Θ represents the TRS operator). Marked in green is the integer quantum Hall effect (IQHE) and marked in red we find

	Symmetry			d								
AZ	TRS	PHS	CS	0	1	2	3	4	5	6	7	8
A	-	-	-	$\mathbb{Z}$	-	$\mathbb{Z}$	-	$\mathbb{Z}$	-	$\mathbb{Z}$	-	$\mathbb{Z}$
AIII	-	-	1	-	$\mathbb{Z}$	-	$\mathbb{Z}$	-	$\mathbb{Z}$	-	$\mathbb{Z}$	-
AI	1	-	-	$\mathbb{Z}$	-	-	-	$\mathbb{Z}$	-	$\mathbb{Z}_2$	$\mathbb{Z}_2$	$\mathbb{Z}$
BDI	1	1	1	$\mathbb{Z}_2$	-	-	-	-	$\mathbb{Z}$	-	$\mathbb{Z}_2$	$\mathbb{Z}_2$
D	-	1	1	$\mathbb{Z}_2$	$\mathbb{Z}_2$	$\mathbb{Z}$	-	-	-	$\mathbb{Z}$	-	$\mathbb{Z}_2$
DIII	-	1	-	-	$\mathbb{Z}_2$	$\mathbb{Z}_2$	$\mathbb{Z}$	-	-	-	$\mathbb{Z}$	-
AII	-1	-	-	$2\mathbb{Z}$	-	$\mathbb{Z}_2$	$\mathbb{Z}_2$	$\mathbb{Z}$		-	-	$\mathbb{Z}$
CII	-1	-1	1	-	$\mathbb{Z}$	-	$\mathbb{Z}_2$	$\mathbb{Z}_2$	$\mathbb{Z}$	-	-	-
C	-	-1	-	-	-	$\mathbb{Z}$	-	$\mathbb{Z}_2$	$\mathbb{Z}_2$	$\mathbb{Z}$	-	-
CI	1	-1	1	-	-	-	$\mathbb{Z}$	-	$\mathbb{Z}_2$	$\mathbb{Z}_2$	$\mathbb{Z}$	-

Table 1: *Table of topological phases classified according to the AZ classification scheme. (Source: Values for d=0 taken from Ref. [12] and for $d > 0$ from Ref. [11].)*

the two-dimensional and three-dimensional topological insulators. Other interesting topologically non-trivial phases can be found in this table, such as, for example, topological superconducting and superfluid phases [11], however not all of the entries have been confirmed by experiments.

We will restrict ourselves to gapped time-reversal invariant systems called "topological insulators", famous for their *gapless* edge states. We have seen, that topologically distinct phases cannot be connected into one another without generating gapless states on the way. We have used an abstract model, but this idea is also valid in real space: If we connect two topologically distinct phases a gapless state has to appear on the edge. Normal insulators, also called trivial insulators, are topologically equivalent to the vacuum, and can thus be smoothly connected to the vacuum. They have accordingly no gapless edge states. TIs, on the other hand, are topologically distinct than the vacuum and a gapless connection is not possible. This is the idea behind

the bulk-edge correspondence. TIs have the additional restriction of TRS, which forces the gapless states to appear in pairs.

1.2 The Integer Quantum Hall Effect

When charged particles in an electrical conductor are deflected by a magnetic field perpendicular to the current, they will accumulate at edges. This will, in turn, induce an electric field perpendicular to both the current and the magnetic field. In equilibrium, $E_{induced} = vB$, current will once more flow through the probe and a finite voltage will exist between the top and bottom edges: This effect is called "Hall effect" after the physicist who discovered it in 1879 [13].

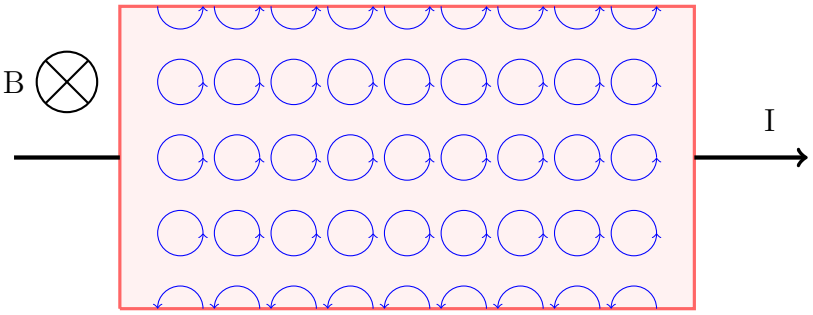

Figure 2: *Explanation of the IQHE in terms of the skipping motion of electrons.*

If the magnetic field is high enough the electrons in the interior of the sample will move in cyclotron orbits, as a result of the Lorentz force. If the sample is very clean, then the electrons will be able to do many orbits before losing the phase coherence and a quantum mechanical treatment is needed [14]. Pictorially, the integer quantum Hall effect can be understood as the skipping motion of electrons at the edge of the probe (see Fig. 2), which explains the chirality of the edge modes and the insulating character of the bulk. In this picture, the chirality of the edge modes is explained by the electron motion being onlu possible in one direction and the isolating

character of the bulk gets explained by the closed cyclotron orbits. It was found in 1980 [15] that the perpendicular conductance takes quantized values of

$$\sigma = n\frac{e^2}{h} \quad \text{for n} \in \mathbb{Z}. \tag{1}$$

The value of n cannot change continuously because it is governed by the topological invariant of the Quantum Hall Effect. Thouless, Kohmoto, Nightingale and den Nijs (TKKN) showed in 1982 [16] that the conductance has the form of an integral over the Berry curvature [11, 17], thus finding an explicit formula for the topological invariant. The number of gapless states in a transition between two regions of different n is determined by the difference of the TKKN invariants and, since the number of states is directly proportional to the conductance, the edge conductance of the IQHE is determined by the topological invariant. Interestingly, the quantization of the Hall conductance has been measured to one part in a billion [18].

1.3 Quantum Spin Hall Insulators

Recently, topological insulators have attracted a lot of attention [11, 17, 19]. This interest comes from the exceptional properties of their boundaries. These edge states are helical and they are protected by time-reversal symmetry, as will be explained below. One expects perfect quantized transport even in the presence of impurities as long as TRS is conserved. These properties make TIs possible candidates for use in Quantum Computers and in the field of spintronics.

The integer quantum Hall effect requires a strong magnetic field and low temperatures. Since a magnetic field is required, TRS is trivially broken. It is, however, not necessary to have broken TRS in order to have a topological class, as we have seen in the zero-dimensional example above. In more physical dimensions, "spin-orbit interaction allows a different topological class of insulating band structures with unbroken TRS" [11, 20]. $\mathbb{Z}_2$-Topological in-

sulators in two dimensions, also known as the quantum spin Hall insulators (QSHI), can be pictorially understood as two copies of the IQHE. However, there is a very important difference. While the edge states in the integer quantum Hall effect are chiral, meaning that they only allow charge transport in one direction, the edge states of quantum spin Hall insulators are helical. Helicity means that there is a lock-in relation between the direction of propagation and the spin of the electrons (see the right panel of Fig. 3).

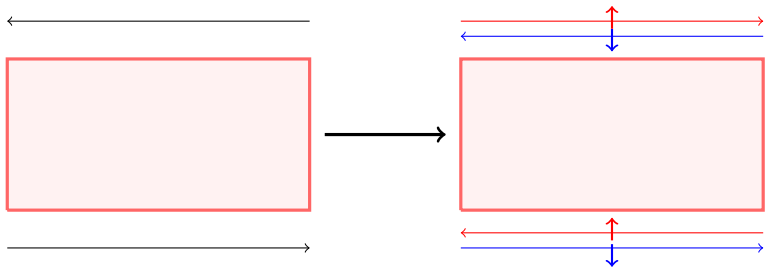

Figure 3: *From the IQHE to quantum spin Hall insulators.*

Another important difference is that, in the integer quantum Hall effect, two edge states having a different direction of propagation are spatially separated by an insulating bulk. This is not the case in a QSHI where each edge hosts states moving in both directions. Chirality of the edge modes in integer quantum Hall effect samples leads to suppression of backscattering. In QSHIs, even when counter-propagating edge states are close, single-particle backscattering by a spinless impurity is still strongly suppressed since the helical modes are protected by time-reversal symmetry.

QSHIs and three-dimensional topological insulators are called $\mathbb{Z}_2$-topological insulators because the topological invariant belongs to $\mathbb{Z}_2$, see Tab. 1. This topological invariant does not have the same interpretation as in the IQHE. There it was related to the conductance of the edges, however, the edge transport in QSHIs is not strictly quantized by the invariant [11, 19].

The $\mathbb{Z}_2$ topological invariant can be understood as the parity of Kramers pairs crossing the bulk gap. Kramers degeneracy of edge states happens at specific points in the Brillouin Zone satisfying the relation $H(\Gamma_i) = \Theta H(\Gamma_i)\Theta^{-}1$.

The number of points that satisfy this relation depends on the form of the lattice. In a 2D square lattice, there are four points satisfying this relationship and in a 3D cubic lattice, there are 8 [17]. It is important that in each of these points, Kramers theorem states that the eigenstates have to be at least doubly degenerate. Consider for simplicity a band with only two Kramers degenerate pairs (see Fig. 4).

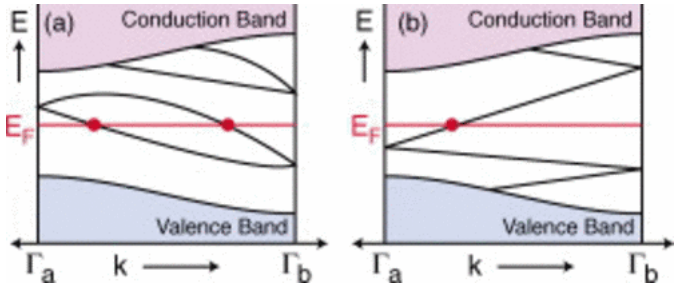

Figure 4: *Electronic dispersion between two points with Kramers degeneracy. The left panel (a) corresponds to a trivial insulator while the right panel (b) corresponds to a topological insulator. (Source: Ref. [11])*

There are two possible ways of connecting Kramers degenerate points: either one connects the same states in both ends or one connects the two states together at one point and with other states at another. In the first case, the number of states crossing the chemical potential is even whereas in the second case the number of states crossing it is odd. One might notice that, in the even case, one can shift the chemical potential up or down and change the system in such a way that no zero-energy crossings occur. In the other case, this is not possible. The second case is equivalent to the existence of topologically protected edge states in a topological insulator and we can relate the topological invariant to the parity of the number of zero-energy crossings.

2 Conductance of edge modes in QSHI

2.1 Experimental and Theoretical Findings

As it has already been stated, QSHIs host gapless edge states and they are predicted to have ideal edge transport, since TRS protects the transport against disorder effects. The conductance of an ideal 1D helical edge should be of $\frac{e^2}{h}$. This has been observed only for small samples [21–24] but experiments performed on longer samples show lower conductance than that expected [21, 23, 25–27]. According to the Landauer-Büttinker formalism [28], lower conductance is a manifestation of backscattering. Another experimental observation [29] in InAs/GaSb quantum wells shows temperature-independent low conductance at low temperatures. This independence is maintained up to 30K.

These experimental findings pose a theoretical puzzle. Under potential disorder, localized bulk electronic states in the gap appear. Potential disorder, however, does not lead to gap openings in the spectrum of the edge modes because it is unable to flip spins [1]. As long as time-reversal symmetry is conserved, models developed to explain the experimental findings may only include inelastic and multi-particle scattering as single-particle backscattering is suppressed. Inelastic processes should generally lead to a strong temperature dependent reduction of conductivity [30–34]. Multi-particle scattering processes are also generally T-dependent [32].

One possible source of the suppressed conductance is the scattering by localized spins (magnetic impurities) in the edge. Two situations are possible: either the total z-component of spin of magnetic impurities and electrons is conserved, i.e. there is a $U(1)$ invariance under rotations of all spins around the z-axis, or this symmetry is not present. $U(1)$ invariance is reflected by XY-isotropic coupling between electrons and impurities.

For single magnetic impurities under $U(1)$ symmetry, it is easy to see that the dc charge transport should not be affected even if backscattering is possible [35]. The reason is represented in Fig. 5, by the fact, that, in order

for the impurity to cause backscattering to a second spin-up electron it has to return to its spin-up state by backscattering a spin-down electron and the dc transport is not affected, because only alternate scattering of right- and left-moving electrons is possible on one edge. Even in the case of a finite density of impurity spins, perfect conductance should be retained as long as $U(1)$ symmetry is present [1, 2].

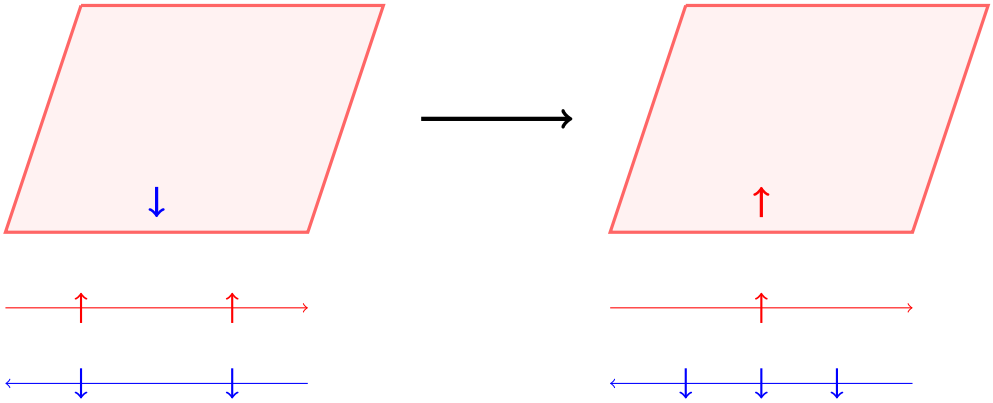

Figure 5: *Illustration of the kinematic reason why $U(1)$ spin-z symmetry does not affect dc conductance. After the backscattering of a spin-up right-moving electron represented here, another backscattering of right-moving electrons is not possible due to $U(1)$ invariance.*

There is, however, no good reason why there should be such $U(1)$ symmetry in disordered systems with spin-orbit interaction [1]. Some $U(1)$ violating processes without spontaneous breaking of time reversal symmetry have been considered in [36–39] but their effects should vanish at low T or weak interaction [1].

2.2 Helical Luttinger Liquid with Randomly Anisotropic Kondo Impurities

Altshuler, Aleiner and Yudson considered in Ref. [1] a chain of localized magnetic impurities at the edge of two-dimensional TIs with randomly anisotropic

coupling of the electrons to the spins. This model was further expanded by Yevtushenko, Wugalter, Yudson and Altshuler in Ref. [2] where the effects of the electron-electron interaction were considered. It has been shown that such randomly anisotropic coupling could lead to a spontaneous breaking of time-reversal symmetry. This removes the symmetry protection and low conductance is expected for low temperature in a broad range of the interaction strength between the electrons. The Hamiltonian describing the model of Refs. [1, 2] reads

$$H_{model} = H_e + H_{int} + H^f_{e-S} + H^b_{e-S}. \tag{2}$$

Where $H_e + H_{int}$ is the Hamiltonian for the interacting Dirac fermions.

$$H_e = -iv_F \int dx \sum_{\mu=\pm} \mu \psi^\dagger_\mu \partial_x \psi^\dagger_\mu \tag{3}$$

$$H_{int} = \frac{g}{2} \int dx \, (\sum_{\mu=\pm} \psi^\dagger_\mu \psi_\mu)^2 \tag{4}$$

The fermionic fields ψ_μ represent spin-up right-moving fermions in the x-direction for $\mu = +$ and spin-down left-moving for $\mu = -$.

$H^f_{e-S} + H^b_{e-S}$ represent the coupling to the Kondo impurities:

$$H^{(f)}_{e-S} = \int dx \; \rho_s J_z S_z (\psi^\dagger_+ \psi_+ - \psi^\dagger_- \psi_-) \tag{5}$$

$$H^{(b)}_{e-S} = \int dx \; \rho_s J_\perp (S^+ e^{2ik_F x} \psi^\dagger_- \psi_+ + \epsilon S^- e^{2ik_F x} \psi^\dagger_- \psi_+ + h.c.) \tag{6}$$

Here H^f_{e-S} represents forward-scattering without spin-flip and H^b_{e-S} represents back-scattering accompanied by spin-flip. We have denoted $J_\perp = (J_x + J_y)/2$ and $\epsilon(x) = (J_x - J_y)/2J_\perp$. $J_\perp$ is the isotropic coupling parameter and ϵ is the dimensionless anisotropy parameter. We consider the case of weak anisotropy $|\epsilon| \equiv a \ll 1$ and a high density of spins and, thus, the coupling terms are expressed with an integral where the dimensionless parameter ρ_s describes the density of spins. It is important to note that one

can, with a unitary transformation, map this system into one with $\tilde{J}_z = 0$ and $\tilde{g} \neq g$ [2]. Accordingly, the model Hamiltonian can be written as

$$H_{model} = H_e + H_{int}[\tilde{g}] + H^{(b)}_{e-S}. \tag{7}$$

Disorder can be introduced into the model by considering a random spin density and anisotropy. Random ρ_s cannot affect dc conductance [1], therefore, it is enough to consider the randomness of the anisotropy parameter, which is taken as a random complex number with Gaussian distribution and zero mean, i.e.

$$\langle \epsilon(x) \rangle = 0 \text{ and } \langle \epsilon(x)\epsilon^*(x) \rangle = \frac{w}{\rho_s}\delta(x - x'). \tag{8}$$

In the noninteracting case, the system can be mapped into the problem of pinning of the helical density wave by the disordered potential. It describes Anderson localization, the phenomenon of localization of waves in a disordered system [40]. In the system under consideration, it takes place for arbitrary weak anisotropy [1].

The authors of Ref. [2] have shown that the localization of edge states takes place in the broad interval of the interaction strength between electrons determined by

$$(\log(E_B\Delta_0))^{-1} < K < 2, \tag{9}$$

where E_B is the UV energy cut-off which is of the order of the bulk gap Δ_0. The interaction leads to strong renormalization of the gap in the electron spectrum Δ and the localization length L_{loc}, which is defined as the lengthscale at which the kinetic energy equals the potential energy of the disorder [41], of

$$\frac{\Delta(K)}{\Delta_0} \sim K\left(\frac{E_B}{K^2\Delta_0}\right) \text{ and } \frac{L_{loc}}{L^{(0)}_{loc}} \sim \left(\frac{\Delta_0}{K\Delta(K)}\right)^{\frac{4}{3}}. \tag{10}$$

Several temperature intervals have been identified. A sample length much smaller than the localization length is expected to have almost ballistic transport with a deviation of the order of L/L_{loc}. On the other hand for samples

that are much longer than the localization length, one has almost zero conductance as long as the temperature is smaller than that of the many-body localization transition [2] as it can be seen in Fig. 6.

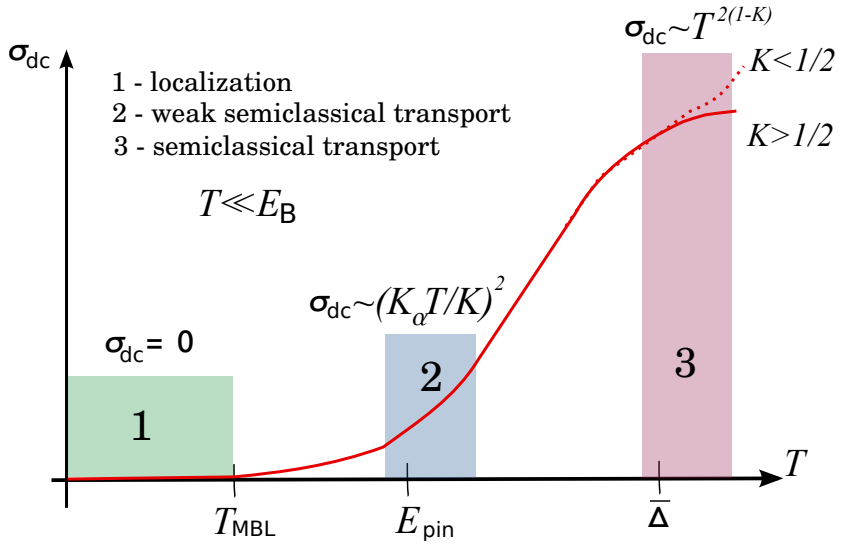

Figure 6: *Qualitative picture of the temperature dependence of the dc conductivity for long samples. (Source: Ref. [2])*

Importantly, the choice of weak anisotropy results in a large localization length. A stronger anisotropy, which might be more physical, would result in smaller L_{loc}, and this might explain the experimental results presented above, especially that of almost temperature-independent localization for low temperatures given in [29].

3 Main Part

3.1 Statement of the Problem

If the helical Kondo array considered in the last section is dense, the direct exchange interaction between the magnetic impurities may be important due to their proximity. The objective of this work is to understand the effects of the direct exchange interaction in the theoretical results presented in the last section. More specifically, we are interested in how the direct exchange interaction changes the localization length of the model. To do this, we add to the Hamiltonian nearest neighbor Heisenberg interaction

$$H_H = J_H \sum_k \vec{S}_k \vec{S}_{k+1}. \tag{11}$$

The sum runs over the magnetic impurities. Here the parameter J_H describes the strength of the Heisenberg interaction and $J_H < 0$ and $J_H > 0$ correspond to the ferromagnetic and antiferromagnetic cases, respectively. For simplicty, we consider an $SU(2)$ symmetric Heisenberg interaction.

3.2 Effective Hamiltonian at $J_H = 0$

In the absence of the Heisenberg interaction, the Hamiltonian is given by Eq. (7). To simplify the model, we will set $\tilde{g}$ to zero. We will later take the effects of the fermionic interaction into account by simply using the renormalized parameters calculated in Ref. [2]. At the first step, we neglect the weak anisotropy, i.e. we set $\epsilon = 0$. The Hamiltonian of the fermions can then be written as

$$H_0 = \int dx\ \psi^\dagger \begin{pmatrix} -iv_F\partial_x & \rho_s J_\perp S^- \\ \rho_s J_\perp S^+ & iv_F\partial_x \end{pmatrix} \psi, \tag{12}$$

where the subscript "0" reflects the fact that the Heisenberg interaction has not yet been taking into account. Here $\psi^\dagger = (\bar{\psi}_+\ ,\ \bar{\psi}_-)$ is the fermionic spinor field. It is important to note that the above formula is obtained after doing

the unitary transformation $S^{\pm} \to S^{\pm} e^{\mp 2ik_F x}$, which leaves the exponential terms containing k_F only in the term that describes the anisotropy in Eq. (6). We use the standard parametrization of the spin variables by unit vectors described by the angle α and by the n_z-component:

$$S^{\pm} = s\sqrt{1 - n_z(x,\tau)^2} e^{\pm i\alpha(x,\tau)}, \tag{13}$$

$$S^{z} = s n_z(x,\tau). \tag{14}$$

We introduce the gap $\tilde{\Delta}_0 = \rho_s J_\perp s\sqrt{1-n_z^2} =: \Delta_0\sqrt{1-n_z^2}$ and rewrite the Hamiltonian as

$$H_0 = \int dx\ \psi^\dagger \begin{pmatrix} -iv_F\partial_x & \tilde{\Delta}_0 e^{-i\alpha} \\ \tilde{\Delta}_0 e^{i\alpha} & iv_F\partial_x \end{pmatrix} \psi. \tag{15}$$

In order to eliminate α from the off-diagonal terms it is convenient to do the gauge transformation given by $\psi_\pm \exp\{\mp i\alpha/2\} \to \psi_\pm$. The Hamiltonian then reads as

$$H_0 = \int dx \left(\psi^\dagger \begin{pmatrix} -iv_F\partial_x - \frac{i}{2}\partial_x\alpha & \tilde{\Delta}_0 \\ \tilde{\Delta}_0 & iv_F\partial_x + \frac{i}{2}\partial_x\alpha \end{pmatrix} \psi + \underbrace{\frac{v_F}{8\pi}(\partial_x\alpha)^2}_{H_{\rm anom}} \right). \tag{16}$$

The new term H_{anom} follows from the Jacobian of the transformation [2]. We can ignore the subleading terms $\pm\frac{i}{2}\partial_x\alpha$, since the spin variable depends on time and space slowly [1, 2]. In particular, the fermionic variables are much faster than α. Focussing in the first part of Eq. (16), we see that it can be written as

$$H' = \int dx\ \psi^\dagger (k v_F \sigma_z + \tilde{\Delta}_0 \sigma_x)\psi. \tag{17}$$

Eq. (17) is the Dirac equation for massive (gapped) fermions. Its dispersion relation, in units of $\hbar = 1$ is given by

$$\omega(k) = \pm\sqrt{(kv_F)^2 + \tilde{\Delta}_0^2}, w \tag{18}$$

see Fig. 7.

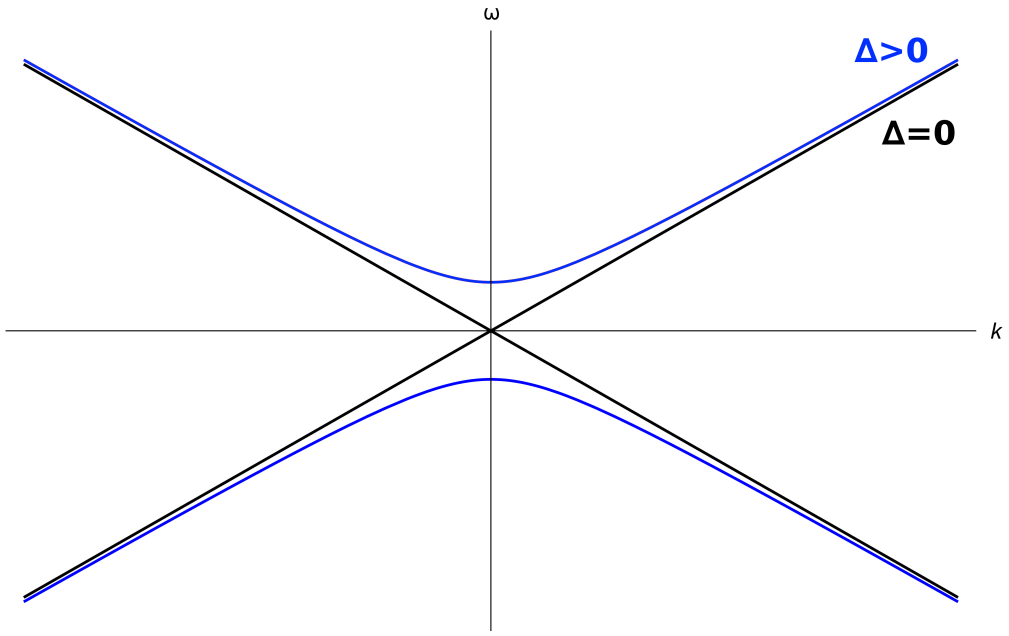

Figure 7: *Dispersion relation for gapped Dirac fermions, where the the chemical potential is set at* $\omega = 0$

We want to know how the gap, created by the electron-spin interactions, changes the energy. To understand this, we subtract the energies given by Eq. (18) to the ones that we have if we set the gap Δ to 0. Next, we use the symmetry of the energies around $k = 0$.

$$\begin{aligned} H_\Delta &= H'|_{\Delta\neq 0} - H'|_{\Delta=0} \\ &= \sum_k \left(-\sqrt{(kv_F)^2 + \tilde{\Delta}_0^2} + v_F k \right) \\ &= 2\sum_{k>0} \left(-\sqrt{(kv_F)^2 + \tilde{\Delta}_0^2} + v_F k \right) \\ &\to 2\int_\Delta^{E_B} dk \frac{L}{2\pi} \left(-\sqrt{(kv_F)^2 + \tilde{\Delta}_0^2} + v_F k \right) \end{aligned} \tag{19}$$

The integration boundary E_B is the so called UV energy cut-off which is of the order of the bulk gap in the TI. This integral can now be calculated (App. B.1) to logarithmic accuracy giving the following result for the energy density:

$$\frac{H_\Delta}{L} = -\frac{1}{2\pi v_F}\tilde{\Delta}_0^2 \log\frac{E_B}{\tilde{\Delta}_0}. \tag{20}$$

3.3 Heisenberg Hamiltonian

The next step is to express the Heisenberg Hamiltonian in terms of variables introduced in the last subsection. At the first step, we consider the spin variables as the mean field approximated spin variables in which we identify n_z and α with their averages and ignore the fluctuations, i.e. $x - \langle x\rangle \to 0$ [42]. Thus, we can equate $\langle n_z^2\rangle$ and $\langle n_z\rangle^2$. A mean field approximation is only valid if the spin variables change slowly in the scale of the lattice spacing ξ_0. In order to be able to effectively describe antiferromagnetic Heisenberg interaction, we need to single out the slow component of S^z. Therefore we introduce the following definition of the spin variables:

$$S_k^\pm = s\sqrt{1-n_z(x_k)^2}e^{\pm i\alpha(x_k)}e^{\mp 2ik_F x_k} \tag{21}$$

$$S_k^z = (-\mathrm{sign}J_H)^k s n_z(x_k) \tag{22}$$

These new definitions do not change the results in the last subsection. One should notice that the factor $e^{\mp 2ik_F x_k}$ appears due to the rotation mentioned above. We insert Eqs. (21) and (22) in the Heisenberg Hamiltonian Eq. (11). The corresponding calculations can be found in App. B.2. This yields

$$H_H \overset{MFA}{=} \frac{L}{\xi_0}\left\{s^2(1-n_z^2)\cos 2k_F\xi_0 - \mathrm{sign}J_H s^2 n_z^2\right\}. \tag{23}$$

We may ignore the constant shift, which only amounts to a shift of the ground state energy and write

$$\begin{aligned}\tilde{H}_H &= -\frac{L}{\xi_0} J_H s^2 (\cos 2k_F\xi_0 + \mathrm{sign} J_H) n_z^2 \\ &= \begin{cases} \frac{L}{\xi_0} J_H s^2 (1 - \cos 2k_F\xi_0) n_z^2, & J_H < 0 \text{ (FM coupling)} \\ -\frac{L}{\xi_0} J_H s^2 (1 + \cos 2k_F\xi_0) n_z^2, & J_H > 0 \text{ (AFM coupling)} \end{cases} \end{aligned} \tag{24}$$

where $n_z^2 = \langle n_z^2 \rangle$.

The whole effective Hamiltonian can thus be written as

$$H_{\text{eff}} = H_\Delta + \tilde{H}_H + H_{\text{anom}} \tag{25}$$

3.4 Fluctuations of the massive spin variable n_z

Minimizing the Hamiltonian with respect to the spin variables results in $n_z = 0, \quad \alpha = \text{const}$, which is the classical configuration of the spin variables. One should, however, notice that this minimum is only found for small values of the Heisenberg parameter J_H. It is expected that at some critical value J_c of J_H, different for the ferromagnetic and anti-ferromagnetic cases, the situation changes. For $|J_H| > |J_c|$ two new minima will appear symmetrically around $n_z = 0$ and $n_z = 0$ will become a maximum (see Fig. 8).

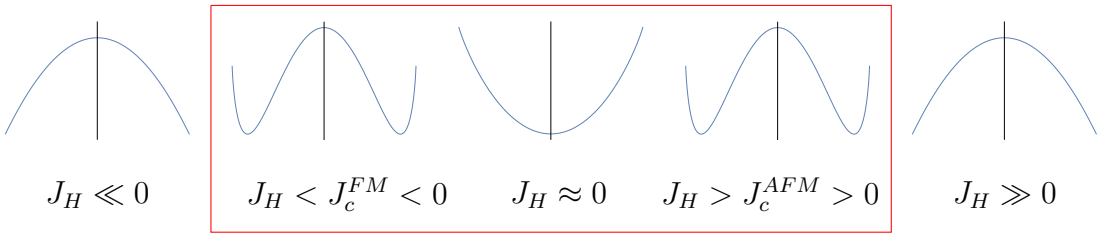

Figure 8: *Dependence of the ground state energy on the spin variable n_z for different values of the Heisenberg parameter J_H.*

This magnetic phase transition lies beyond the scope of this text and will therefore not be studied here. At very high $|J_H|$, the Heisenberg in-

teraction will dominate the ground state energy, which is also beyond our consideration.

Now, we expand H_Δ around $n_z = 0$ up to second order arriving at an expression valid for $|J_H| \ll J_c$

$$\begin{aligned} H_\Delta &\approx \frac{L}{2\pi v_F}\Delta_0^2(\log\left(\frac{E_B}{\Delta_0}\right) - \frac{1}{2})n_z^2 \\ &\approx \frac{L}{2\pi v_F}\Delta_0^2 \log\left(\frac{E_B}{\Delta_0}\right)n_z^2 \end{aligned} \tag{26}$$

Here, $n_z^2 = \langle n_z^2 \rangle$. The last approximation is valid because the logarithm is large. Using $\langle n_z^2 \rangle = \frac{1}{L}\int dx (n_z^2)$ we can see that

$$H_\Delta + \tilde{H}_H \approx \int dx \underbrace{\left(\frac{\Delta_0^2}{2\pi v_F} \log\left(\frac{E_B}{\Delta_0}\right) - \frac{J_H s^2}{\xi_0}(\cos 2k_F\xi_0 + \mathrm{sign} J_H)\right)}_{=:\mathcal{P}(\Delta_0, J_H)} n_z^2. \tag{27}$$

This approximation is only valid at small J_H far from the phase transition as we have expanded around $n_z = 0$. This Hamiltonian describes small fluctuations of the massive spin variable n_z around this minimum. We therefore name the RHS of Eq. (27) H_{FL}. The Hamiltonian Eq. (25) now reads as

$$H_{eff} = H_{FL} + H_{anom} = \int dx \ \left(\mathcal{P} n_z^2 + \frac{1}{8\pi v_F}(\partial_x \alpha)^2 \right). \tag{28}$$

3.5 Effective Lagrangian for Spinons

We now change from the Hamiltonian representation to the Lagrangian representation, because it allows to explicitly take the effects of the fluctuations of n_z into account. We take the fermionic interactions explicitly into account by using the renormalized parameters calculated in Ref. [2]: We subsitute the effective gap Δ (see Eq. (10)) for the bare gap Δ_0 in $\mathcal{P}$ and the renormalized factor $v/8\pi K$ in H_{anom}. We also recover the anisotropy: It is given by adding the term $-\mathcal{D}(\epsilon e^{2i\alpha} + h.c.)$ to the Lagrangian (see Ref. [2]), where

$D = \frac{1}{4\pi a}\frac{\Delta}{E_B}\log\frac{E_B}{\Delta}$ and $a \sim v_F/E_B$ is the smallest spatial scale. The Lagrangian is given by

$$\mathcal{L} = \mathcal{L}_{FL}[n_z] + \mathcal{L}_{anom}[\alpha] + \mathcal{L}_{WZ}[n_z, \alpha] - \mathcal{D}(\epsilon e^{2i\alpha} + h.c.), \tag{29}$$

where

$$\mathcal{L}_{FL}[n_z] = \mathcal{P}(\Delta, J_H) n_z^2, \tag{30}$$

$$\mathcal{L}_{anom} = \frac{v}{8\pi K}(\partial_x \alpha)^2, \tag{31}$$

$$\mathcal{L}_{WZ} = -is\rho_s n_z \rho_\tau \alpha. \tag{32}$$

$\mathcal{L}_{WZ}$ is the so-called Wess-Zumino term, which is needed when the spins are parametrized by unit vectors [43].

In order to derive the effective action for the spinons we need to integrate out the massive variable n_z and, since it is massive, we can extend the integration measure so as to calculate the integral in the Gaussian approximation. It is coupled to the massless phase α in the Wess-Zumino term, and therefore the Gaussian integral over n_z, which can be found in App. B.3, yields:

$$\left\langle e^{-S_{WZ}} \right\rangle_{S_{FL}} = \exp\left(-\frac{s^2}{2} \int dx \int d\tau \rho_s^2 \left\langle n_z^2 \right\rangle_{S_{FL}} (\partial_\tau \alpha)^2 \right), \tag{33}$$

$$\text{where } \left\langle n_z^2 \right\rangle_{S_{FL}} = (2\mathcal{P})^{-1}. \tag{34}$$

We rewrite the non-anisotropic terms of the Lagrangian in terms of the Lagrangian for the Luttinger liquid (see App. A) with new paramers v_α and K_α. The Lagrangian for the Luttinger liquid is given by

$$\mathcal{L}_{LL}[\phi, K, v] = \frac{1}{2\pi K v}\left[(\partial_\tau \phi)^2 + (v\partial_x \phi)^2\right]. \tag{35}$$

We now have

$$\mathcal{L}_{anom}[\alpha] + \frac{(s\rho_s)^2}{2}\left\langle n_z^2 \right\rangle_{S_{FL}} (\partial_\tau \alpha)^2 \stackrel{!}{=} \mathcal{L}_{LL}[\alpha, K_\alpha, v_\alpha]. \tag{36}$$

This, in turn, gives us two equations for the parameters K_α and v_α which read as follows

$$\frac{1}{2\pi K_\alpha v_\alpha} = \frac{(s\rho_s)^2}{2}\left\langle n_z^2 \right\rangle_{S_{FL}} \quad \text{and} \quad \frac{v_\alpha}{2\pi K_\alpha} = \frac{v}{8\pi K}. \tag{37}$$

Eq. (37) shows how the rigidity of the collective helical mode is modified by the direct exchange.

The effective Lagrangian for the fluctuations of the spin phase α is then given by

$$\mathcal{L}_\alpha = \mathcal{L}_{LL}[\alpha, K_\alpha, v_\alpha] - D(\epsilon e^{2i\alpha} + h.c.). \tag{38}$$

3.6 Localization Length

We now use Eq. (38), where the anisotropy parameter ϵ is described by Eq. (8), to calculate the localization length L_{loc} using the optimization methods described in Sect.9.2 in [41]. We assume that the phase α remains constant on the lengthscale L_{loc} and estimate the energy of the disorder as $\mathcal{D}\sqrt{\frac{\omega}{\rho_s}L_{loc}}$, because the average of a gaussian random variable grows with the square root of the length over which it is integrated. We focus in the case where the temperature is very small $T \to 0$ and neglect the time derivatives $\partial_\tau \alpha$, because the fluctuations of α are frozen out at $K_\alpha \to 0$ (semiclassics). The constant value taken by the phase is that which optimizes the disorder term in the interval L_{loc}. Between two segments of L_{loc} the phase α has to change in order to reach the next minimum (see Fig. 9), and we can estimate the gradient of the phase to be $\partial_x \alpha \sim 1/L_{loc}$ and therefore the kinetic energy as $v/L_{loc}K$.

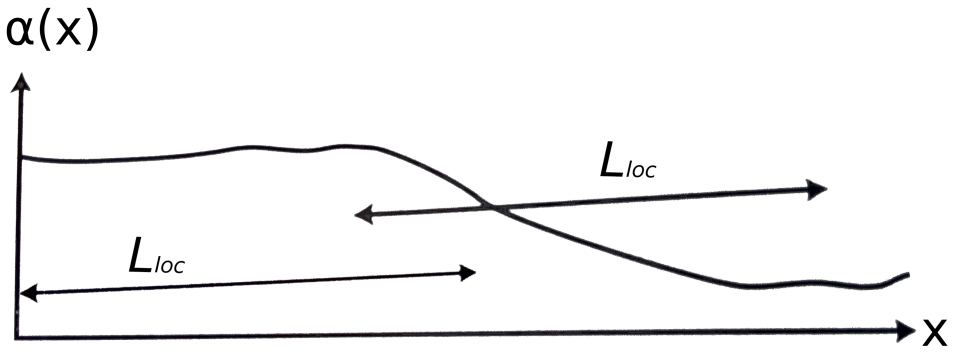

Figure 9: *The phase α takes the value which optimizes the disorder term over a length L_{loc}, which is given by the lengthscale at which the kinetic energy equals the potentail energy of the disorder. (Source: Adapted from Ref. [41])*

As it has already been stated in section 2.2, the localization length is defined as the lengthscale at which the kinetic energy equals the potential energy of the disorder. We therefore find using the relationships $vK = v_F \sim aE_B$ and $\rho_s a \sim 1$ (the second describes dense impurities, which is the regime we study)

$$\frac{v}{L_{loc}K} \sim \mathcal{D}\sqrt{\frac{\omega}{\rho_s}L_{loc}} \implies L_{loc} \sim \frac{a}{\omega^{1/3}}\left(\frac{E_B}{a\mathcal{D}K^2}\right)^{2/3}. \tag{39}$$

One should note that this is the same expression found in Ref. [2] without considering the direct exchange interaction. This shows that the theory is robust against weak $SU(2)$ symmetric Heisenberg interaction. Let us now verify the validity of the calculations.

This approach is only valid if $K_\alpha \to 0$, which corresponds to a strong effective repulsion because the spinons couple strongly to the interacting fermions. It is therefore important to make sure that this limit is still valid if one introduces the Heisenberg interaction. We now examine the dependance of K_α on the Heisenberg parameter J_H. In order to do this we solve Eq. (37)

for K_α and find

$$K_\alpha = \frac{2}{s\rho_s}\sqrt{\frac{K}{\pi v \langle n_z^2\rangle_{S_{FL}}}} \propto \left\langle n_z^2 \right\rangle_{S_{FL}}^{-\frac{1}{2}} \propto \sqrt{\mathcal{P}}. \tag{40}$$

K_α was found to be very small in the absence of the Heisenberg interaction. It is easy to see in Eq. (27) that $\mathcal{P}$ gets smaller with increasing $|J_H|$. One can, therefore, follow that the Heisenberg interaction makes K_α smaller and thus the limit $K_\alpha \to 0$ even more valid. We see accordingly that Eq. (39) remains valid even in the presence of weak Heisenberg.

4 Conclusion and Outlook

In this work, we have studied the effect of $SU(2)$ symmetric nearest-neighbor direct exchange on tranport in a helical Luttinger Liquid coupled to randomly anisotropic Kondo impurities. This model is relevant for the edge transport in time reversal invariant topological insulators [1, 2]. We have found that such $SU(2)$ symmetric Heisenberg interaction is unable to change the localization length if the Heisenberg interaction couping is small. A strong Heisenberg interaction is expected to lead the system towards a magnetic phase transition [44].

We have arrived at this conclusion by deriving an effective Lagrangian describing the low energy theory for a helical colletive (electron - Kondo spin) mode which supports the charge transport and then using standard optimization procedures to evaluate the localization length.

We believe that the robustness of the localization length is a result of the choice of $SU(2)$ symmetric Heisenberg interaction. In order to understand the effects of anisotropic (and probably random) interaction between the magnetic impurities further work is required. We have also analysed how the rigidity of the collective helical mode is modified by the direct exchange. This might be a useful input for a further theory addressing the ac-response of the system.

Acknowledgment

I am indebted to Prof. Jan von Delft and the LS von Delft for the opportunity to do this Bachelor thesis under astounding working conditions.

I would like to express my gratitude to my supervisor Oleg Yevtushenko for coming up with the project and for everything he has taught me. I am particularly grateful to him for having introduced me to the wonderful world of low-dimensional condensed matter physics.

Needless to say, I also am much obliged to friends and family for their time and support over the years.

A Luttinger Liquids

In the Luttinger model, one linearizes the dispersion relation of the electrons close to the Fermi energy. In order to quantitatively understand Luttinger Liquids (LL) one has to resort to methods such as bosonization, which lay behind the scope of this text. It is a mathematical procedure in (1+1) dimensions in which interacting fermions are treated as massless, non-interacting bosons. A review of bosonization can be found at [45]. It is important to consider that in such a case one has to consider left and right moving particles close to $\pm k_F$ separately. One of the most important results of bosonization is that the Hamiltonian and the action for the spinless Luttinger liquid can be written as [41]

$$H = \frac{\hbar}{2\pi} \int dx \left[\frac{vK}{\hbar^2} (\pi \Pi(x))^2 + \frac{v}{K} (\nabla \phi(x))^2 \right] \tag{41}$$

$$S/\hbar = \frac{1}{2\pi v K} \int dz \left[(\partial_\tau \phi)^2 + (v \partial_x \phi)^2 \right] \tag{42}$$

for free scalar field ϕ and momentum Π, where ϕ and Π obey the canonically conjugate commutation rule for bosons. This Hamiltonian describes a free boson model with effective velocity v and stiffness K, better known as the Luttinger parameter. The bosons in question represent the density fluctuations of the interacting fermions and thus the velocity v indicates the propagation velocity of said fluctuations. The Luttinger parameter represents the type of interaction between the fermions: $K > 1$ corresponds to attractive interactions whereas $K < 1$ corresponds to repulsive interactions.

When spin is considered the Hamiltonian separates into spin and charge with different stiffness K and propagation velocity v for spin and charge density fluctuations. This is known as spin-charge separation and it is one of the hallmarks of Luttinger liquids. In the helical model considered in this work, however, such a separation does not take place because helicity fixes spin and propagation.

B Some Explicit Calculations

B.1 Calculation of H_Δ

In Eq. (19) we arrived at the following expression for H_Δ:

$$H_\Delta \approx 2\int_\Delta^{E_B} dk \frac{L}{2\pi}\left(-\sqrt{(kv_F)^2+\Delta^2}+kv_F\right). \tag{43}$$

We now perform the change of variables given by $\epsilon = kv_F$ and so

$$\begin{aligned} H_\Delta \approx & 2\frac{L}{2\pi}\int_\Delta^{E_B} dk \left(-\sqrt{(kv_F)^2+\Delta^2}+kv_F\right) \\ = & 2\frac{L}{2\pi v_F}\int_{\Delta v_F}^{E_B v_F} d\epsilon(\epsilon-\sqrt{\epsilon^2+\Delta^2}) \\ = & 2\frac{L}{2\pi v_F}\int_{\Delta v_F}^{E_B v_F} d\epsilon(\epsilon-\epsilon\sqrt{1+(\frac{\Delta}{\epsilon})^2}) \end{aligned} \tag{44}$$

Here, interestingly, $\frac{1}{2\pi v_F}$ corresponds to the one-dimensional density of states. We now expand the square root with $\sqrt{1+x^2} = 1+\frac{1}{2}x^2+O(x^3)$ and find:

$$\begin{aligned} H_\Delta \approx & 2\frac{L}{2\pi v_F}\int_{\Delta v_F}^{E_B v_F} d\epsilon(\epsilon-\epsilon(1+\frac{1}{2}(\frac{\Delta}{\epsilon})^2)) \\ = & -\frac{L}{2\pi v_F}\int_{\Delta v_F}^{E_B v_F} d\epsilon\frac{\Delta^2}{\epsilon} \\ = & -\frac{L}{2\pi v_F}\Delta^2\log\frac{E_B}{\Delta}. \end{aligned} \tag{45}$$

Which is the expression given in Eq. (20).

B.2 Calculation of H_H

We now want to derive Eq. (23). For this we start with the Heisenberg Hamiltonian given by

$$H_H = J_\perp \sum_k \vec{S}_k\vec{S}_{k+1} \tag{46}$$

As usual, we introduce ladder operators defined by $S^{\pm} = S^x \pm iS^y$. One can show, after some algebra, that under this definition, the following expression holds true:

$$S_k^x S_{k+1}^x + S_k^y S_{k+1}^y = \frac{1}{2}(S_k^+ S_{k+1}^- + S_k^- S_{k+1}^+) \tag{47}$$

and, using the expression for the spin variables Eqs. (21) and (22), the Heisenberg Hamiltonian can be rewritten as

$$\begin{aligned}
H_H =& J_H \sum_k \frac{1}{2}(S_k^+ S_{k+1}^- + S_k^- S_{k+1}^+) + S_k^z S_{k+1}^z \\
=& J_H \sum_k \frac{1}{2} s^2 \sqrt{1 - n_z^2(x_k)}\sqrt{1 - n_z^2(x_{k+1})}(e^{-i(\alpha(x_{k+1}) - \alpha(x_k))} e^{+2ik_F(x_{k+1} - x_k)} + h.c.) \\
& - \text{sign}(J_H) s^2 n_z(x_k) n_z(x_{k+1}) \\
=& J_H \sum_k s^2 \sqrt{1 - n_z^2(x_k)}\sqrt{1 - n_z^2(x_{k+1})} \cos(2k_F(x_{k+1} - x_k) - (\alpha(x_{k+1}) - \alpha(x_k))) \\
& - \text{sign}(J_H) s^2 n_z(x_k) n_z(x_{k+1}) \\
\overset{\text{MFA}}{=}& J_H \sum_k s^2(1 - n_z^2)\cos(2k_F\xi_0) - \text{sign}(J_H) s^2 n_z^2,
\end{aligned} \tag{48}$$

where $\xi_0 = x_{k+1} - x_k$ and n_z corresponds to its expectation value. Interestingly, all the dependence of the Hamiltonian on α gets lost after the mean-field approximation. Since n_z corresponds to the average, there is no dependence on the index k and we can multiply by the number of impurities N. It is given by the length of the sample L divided by the average distance between subsequent impurities, which corresponds to ξ_0 if one assumes a homogeneous distribution of the impurities.

$$\begin{aligned}
H_H \overset{\text{MFA}}{=}& J_H N \left\{ s^2(1 - n_z^2)\cos(2k_F\xi_0) - \text{sign}(J_H) s^2 n_z^2 \right\} \\
=& J_H \frac{L}{\xi_0} \left\{ s^2(1 - n_z^2)\cos(2k_F\xi_0) - \text{sign}(J_H) s^2 n_z^2 \right\}
\end{aligned} \tag{49}$$

We can now ignore the constant shift given by $J_H L/\xi_0 s^2 \cos 2k_F\xi_0$ and arrive at Eq. (24):

$$\tilde{H}_H = -J_H \frac{L}{\xi_0} s^2 \left\{ \text{sign}(J_H) + \cos(2k_F \xi_0) \right\} \tag{50}$$

B.3 Fluctuations Average of the Wess-Zumino Action

If the Heisenberg interaction is weak, the action describing the fluctuations of the massive spin variable n_z has the form

$$S_{FL}[n_z] = \int dz \ \mathcal{P} \ n_z^2 \tag{51}$$

where the prefactor $\mathcal{P}(\Delta, J_H)$ is given by

$$\frac{\Delta^2}{2\pi v_F} \log \frac{E_B}{\Delta} - \frac{J_H s^2}{\xi_0} (\cos 2k_F \xi_0 + \text{sign} J_H) \tag{52}$$

We can now calculate an effective action for the Wess-Zumino term:

$$\left\langle e^{-S_{WZ}} \right\rangle_{S_{FL}} = \left\langle e^{+is \int dz \rho_s n_z \partial_\tau \alpha} \right\rangle_{S_{FL}} \tag{53}$$

$$= \frac{\int \mathcal{D} n_z e^{+is \int dz \rho_s n_z \partial_\tau \alpha} e^{- \int dz p n_z^2}}{\int \mathcal{D} n_z e^{- \int dz p n_z^2}} \tag{54}$$

This can be calculated by completing the square:

$$is\rho_s \partial_\tau \alpha n_z - p n_z^2 = -p(\underbrace{(n_z - \frac{is\rho_s \partial_\tau \alpha}{2p})}_{\tilde{n}_z}^2) - (\frac{is\rho_s \partial_\tau \alpha}{2p})^2) \tag{55}$$

And accordingly

$$\left\langle e^{-S_{WZ}} \right\rangle_{S_{FL}} = \frac{\int \mathcal{D} \tilde{n}_z e^{- \int dz \mathcal{P} \tilde{n}_z^2} e^{-\frac{s^2}{2} \int dz \rho_s^2 (2\mathcal{P})^{-1} (\partial_\tau \alpha)^2}}{\int \mathcal{D} n_z e^{- \int dz \mathcal{P} n_z^2}} \tag{56}$$

$$= \exp\left(-\frac{s^2}{2} \int dz \rho_s^2 (2\mathcal{P})^{-1} (\partial_\tau \alpha)^2 \right) \tag{57}$$

One might notice that $(2\mathcal{P})^{-1} = \langle n_z^2 \rangle_{S_{FL}}$: This can be calculated by using the relationship given by

$$\left\langle n_z^2 \right\rangle_{S_{FL}} = \frac{1}{Z[0]} \frac{\partial^2 Z[J]}{\partial J^2}|_{J=0} \tag{58}$$

where the partition function is given by $Z[J] = \int \mathcal{D}n_z e^{-S_{FL} - \int dz J n_z}$. By completing the square and deriving twice for J one arrives at the aforementioned relation $(2\mathcal{P})^{-1} = \langle n_z^2 \rangle_{S_{FL}}$.

We can now insert this last relation into Eq. (57) and find

$$\left\langle e^{-S_{WZ}} \right\rangle_{S_{FL}} = \exp\left(-\frac{s^2}{2} \int dz \rho_s^2 \left\langle n_z^2 \right\rangle_{S_{FL}} (\partial_\tau \alpha)^2 \right). \tag{59}$$

References

[1]B. L. Altshuler, I. L. Aleiner, and V. I. Yudson, "Localization at the Edge of a 2D Topological Insulator by Kondo Impurities with Random Anisotropies", Physical Review Letters **111**, 086401, 086401 (2013).

[2]O. M. Yevtushenko, A. Wugalter, V. I. Yudson, and B. L. Altshuler, "Transport in helical Luttinger Liquid with Kondo impurities", EPL Journal **112** (2015) 10.1209/0295-5075/112/57003.

[3]A. Akhmerov, J. Sau, B. van Heck, S. Rubbert, R. Skolasiński, B. Nijholt, I. Muhammad, and T. Ö. Rosdahl, *Topology in Condensed Matter Physics: Topology and symmetry*, https://topocondmat.org/w1_topointro/0d.html, Accessed: 2017.

[4]H. Kramers, "Théorie générale de la rotation parmagnétique dans les cristaux", Proceedings Koninklijke Akademie van Wetenschappen (1930).

[5]E. Wigner, "Über die Operation der Zeitumkehr in der Quantemechanik", Nachrichten von der Gesellschaft der Wissenschaften zu Göttingen (1932).

[6]A. P. Schnyder, S. Ryu, A. Furusaki, and A. W. W. Ludwig, "Classification of Topological Insulators and Superconductors in Three Spatial Dimensions", Phys. Rev. B **78**, 195125 (2008).

[7]A. Kitaev, "Periodic Table for Topological Insulators and Superconductors", American Institute of Physics Conference Series **1134**, edited by V. Lebedev, and M. Feigel'Man, 22–30 (2009).

[8]A. P. Schnyder, S. Ryu, A. Furusaki, and A. W. W. Ludwig, "Classification of Topological Insulators and Superconductors", American Institute of Physics Conference Series **1134**, edited by V. Lebedev, and M. Feigel'Man, 10–21 (2009).

[9]S. Ryu, A. P. Schnyder, A. Furusaki, and A. W. W. Ludwig, "Topological Insulators and Superconductors: Tenfold Way and Dimensional Hierarchy", New Journal of Physics **12**, 065010, 065010 (2010).

[10]A. Altland, and M. R. Zirnbauer, "Nonstandard Symmetry Classes in Mesoscopic Normal-superconducting Hybrid Structures", Phys. Rev. B **55**, 1142–1161 (1997).

[11]M. Hasan, and C. Kane, "Colloquium: Topological Insulators", Reviews of modern physics **82**, 3045–3067 (2010).

[12]J. Väyrynen, "The Gradient Expansion and Topological Insulators", MA thesis (University of Helsinki, 2011).

[13]E. H. Hall, "On a new action of the magnet on electric currents.", American Journal of Mathematics (1879) `10.2307/2369245`.

[14]A. J. Bestwick, "Quantum Edge Transport in Topological Insulators", PhD thesis (Stanford University, 2015).

[15]K. v. Klitzing, G. Dorda, and M. Pepper, "New Method for High-Accuracy Determination of the Fine-Structure Constant Based on Quantized Hall Resistance", Phys. Rev. Lett. **45**, 494–497 (1980).

[16]D. J. Thouless, M. Kohmoto, M. P. Nightingale, and M. den Nijs, "Quantized Hall Conductance in a Two-Dimensional Periodic Potential", Phys. Rev. Lett. **49**, 405–408 (1982).

[17]S.-Q. Shen, *Topolgical Insulators. Dirac Equation in Condensed Matters*, Springer Series in Solid-State Sciences (Springer, 2012).

[18]K. von Klitzing, "Developments in the Quantum Hall Effect", Philosophical Transactions of the Royal Society of London A: Mathematical, Physical and Engineering Sciences **363**, 2203–2219 (2005).

[19]X.-L. Qi, and S.-C. Zhang, "Topological Insulators and Superconductors", Reviews of modern physics **83**, 1057–1110 (2011).

[20]C. L. Kane, and E. J. Mele, "Quantum Spin Hall Effect in Graphene", Phys. Rev. Lett. **95**, 226801 (2005).

[21]M. König, S. Wiedmann, C. Brüne, A. Roth, H. Buhmann, L. Molenkamp, X.-L. Qi, and S.-C. Zhang, "Quantum Spin Hall Insulator State in HgTe Quantum Wells", Science **318**, 766 (2007).

[22]A. Roth, C. Brüne, H. Buhmann, L. W. Molenkamp, J. Maciejko, X.-L. Qi, and S.-C. Zhang, "Nonlocal Transport in the Quantum Spin Hall State", Science **325**, 294 (2009).

[23]L. Du, I. Knez, G. Sullivan, and R.-R. Du, "Observation of Quantum Spin Hall States in InAs/GaSb Bilayers under Broken Time-Reversal Symmetry", ArXiv e-prints (2013).

[24]K. Suzuki, Y. Harada, K. Onomitsu, and K. Muraki, "Edge channel Transport in the InAs/GaSb Topological Insulating Phase", Physical Review B **87**, 235311, 235311 (2013).

[25]I. Knez, R.-R. Du, and G. Sullivan, "Evidence for Helical Edge Modes in Inverted InAs/GaSb Quantum Wells", Phys. Rev. Lett. **107**, 136603 (2011).

[26]G. Grabecki, J. Wróbel, M. Czapkiewicz, Ł. Cywiński, S. Gierałtowska, E. Guziewicz, M. Zholudev, V. Gavrilenko, N. N. Mikhailov, S. A. Dvoretski, F. Teppe, W. Knap, and T. Dietl, "Nonlocal Resistance and its Fluctuations in Microstructures of Band-Inverted HgTe/(Hg,Cd)Te Quantum Wells", Physical Review B **88**, 165309, 165309 (2013).

[27]I. Knez, C. T. Rettner, S.-H. Yang, S. S. P. Parkin, L. Du, R.-R. Du, and G. Sullivan, "Observation of Edge Transport in the Disordered Regime of Topologically Insulating InAs/GaSb Quantum Wells", Phys. Rev. Lett. **112**, 026602 (2014).

[28]Y. V. Nazarov, and Y. M. Blanter, *Quantum Transport: Introduction to Nanoscience* (Cambridge University Press, 2009).

[29]E. M. Spanton, K. C. Nowack, L. Du, G. Sullivan, R.-R. Du, and K. A. Moler, "Images of Edge Current in InAs /GaSb Quantum Wells", Physical Review Letters **113**, 026804, 026804 (2014).

[30]F. Crépin, J. Budich, F. Dolcini, P. Recher, and B. Trauzettel, "Renormalization Group Approach for the Scattering off a Single Rashba Impurity in a Helical Liquid", Physical Review B **86**, 121106, 121106 (2012).

[31]T. L. Schmidt, S. Rachel, F. von Oppen, and L. I. Glazman, "Inelastic Electron Backscattering in a Generic Helical Edge Channel", Phys. Rev. Lett. **108**, 156402 (2012).

[32]N. Lezmy, Y. Oreg, and M. Berkooz, "Single and Multiparticle Scattering in Helical Liquid with an Impurity", Phys. Rev. B **85**, 235304 (2012).

[33]J. I. Väyrynen, M. Goldstein, and L. I. Glazman, "Helical Edge Resistance Introduced by Charge Puddles", Phys. Rev. Lett. **110**, 216402 (2013).

[34]J. I. Väyrynen, M. Goldstein, Y. Gefen, and L. I. Glazman, "Resistance of Helical Edges Formed in a Semiconductor Heterostructure", Phys. Rev. B **90**, 115309, 115309 (2014).

[35]Y. Tanaka, A. Furusaki, and K. A. Matveev, "Conductance of a Helical Edge Liquid Coupled to a Magnetic Impurity", Physical Review Letters **106**, 236402, 236402 (2011).

[36]J. Maciejko, "Kondo Lattice on the Edge of a Two-Dimensional Topological Insulator", Phys. Rev. B **85**, 245108, 245108 (2012).

[37]V. Cheianov, and L. I. Glazman, "Mesoscopic Fluctuations of Conductance of a Helical Edge Contaminated by Magnetic Impurities", Physical Review Letters **110**, 206803, 206803 (2013).

[38]B. Braunecker, P. Simon, and D. Loss, "Nuclear Magnetism and Electron Order in Interacting One-Dimensional Conductors", Phys. Rev. B **80**, 165119, 165119 (2009).

[39]A. Del Maestro, T. Hyart, and B. Rosenow, "Backscattering Between Helical Edge States via Dynamic Nuclear Polarization", Phys. Rev. B **87**, 165440 (2013).

[40]P. W. Anderson, "Absence of Diffusion in Certain Random Lattices", Physical Review **109**, 1492–1505 (1958).

[41]T. Giamarchi, *Quantum Physics in One Dimension*, International Series of Monographs on Physics (Oxford University Press, 2003).

[42]U. Schollwöck, *T_M1/TV: Advanced Statistical Physics (Statistical Physics II), Chapter 5: Mean-Field Theory*, `http://www.physik.uni-muenchen.de/lehre/vorlesungen/sose_14/asp/lectures/index.html`, Accessed: 2017.

[43]A. Altland, and B. Simons, *Condensed Matter Field Theory* (Cambridge University Press, 2006).

[44]O. Yevtushenko, and A. Tsvelik, "Supersolid Magnetic Order on Edge of Quantum Spin Hall Samples", (In progress, 2017).

[45]J. von Delft, and H. Schoeller, "Bosonization for Beginners — Refermionization for Experts", Annalen der Physik **7**, 225–305 (1998).

Erklärung

Hiermit erkläre ich, die vorliegende Arbeit selsbständig verfasst zu haben und keine anderen als die in der Arbeit angegebenen Quellen und Hilfsmittel benutzt zu haben.
München, 08. September 2017

Pol Alonso-Cuevillas Ferrer